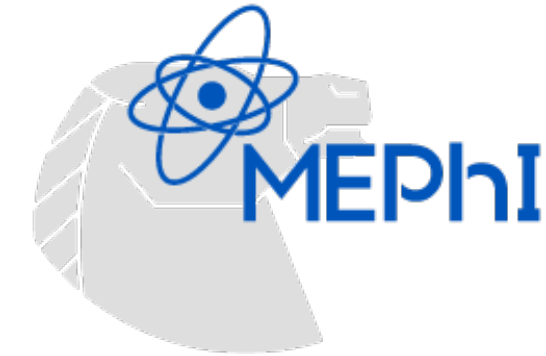


ИССЛЕДОВАНИЕ КЛАСТЕРНОЙ СТРУКТУРЫ АТОМНЫХ ЯДЕР И ЕЁ ПРОЯВЛЕНИЙ В ЯДЕРНЫХ РЕАКЦИЯХ



Бажин Антон Сергеевич

1.3.15 Физика атомных ядер и элементарных
частиц, физика высоких энергий

Кафедра № 40 «Физика элементарных частиц»

Научный руководитель: д.ф-м.н. Гуров Юрий Борисович

Консультант: д.ф-м.н Самарин Вячеслав Владимирович

2025, Москва

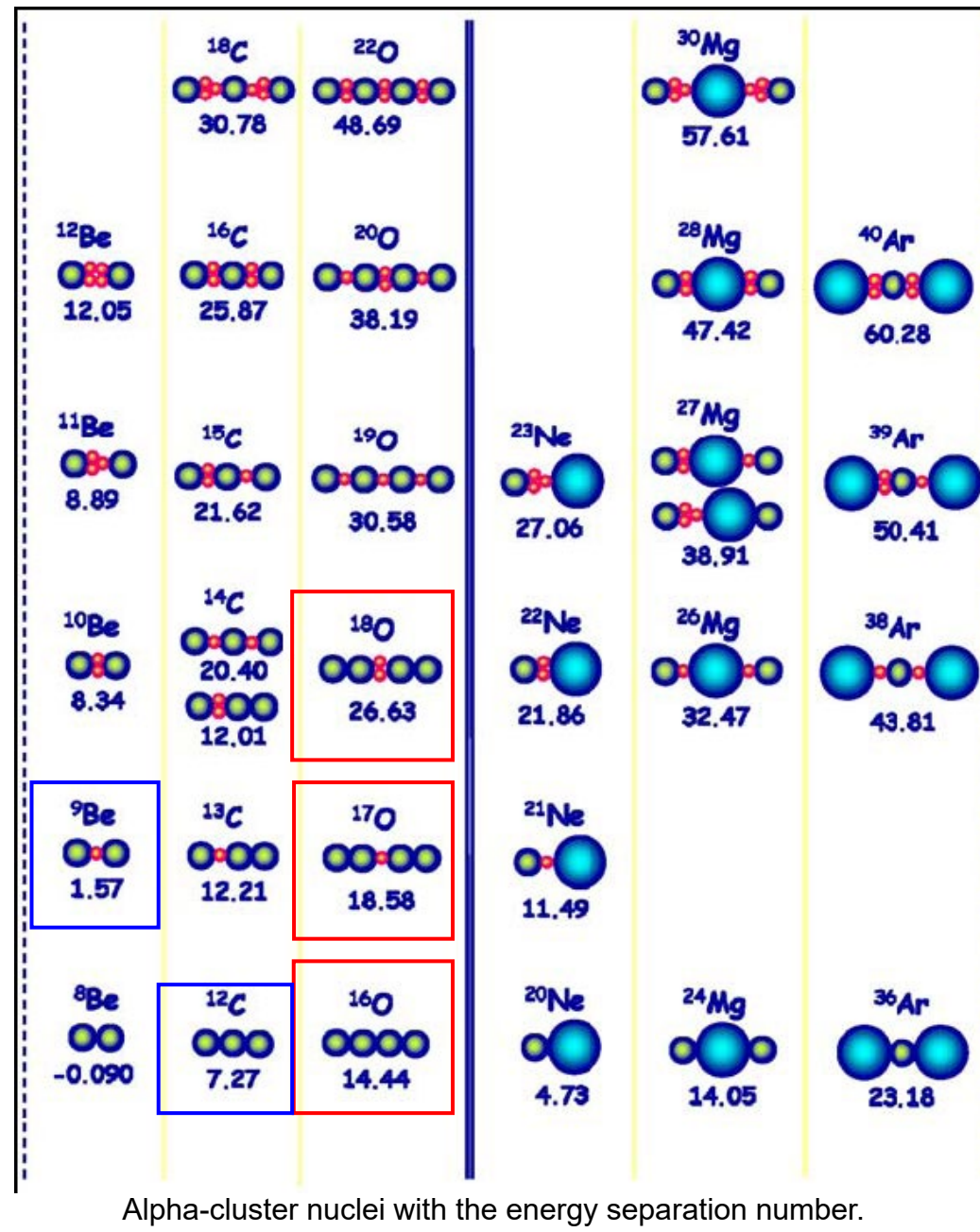
Общий план работы

1. Разработка методов для изучения структуры кластерных ядер: метод функций Йоста, метод Фейнмана по траекториям, метод гиперсферических функций.
2. Изучение структуры альфа-кластерных ядер на основе их экспериментальных данных. Проведено исследование ядер ${}^9\text{Be}$, ${}^6\text{Li}$, ${}^{12}\text{C}$, ${}^{18}\text{O}$ и ${}^{16}\text{O}$.
3. Использование полученных пространственных структур в расчётах ядерных реакций с помощью метода DWBA.

In the recent time there was rising interest in the study of neutron-rich and exotic weakbound nuclei – exotic cluster structures (see, for example, [1]).

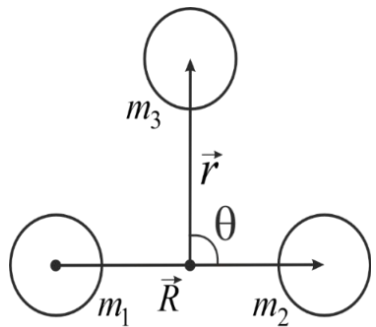
[1] W. von Oertzen, M. Freer, Y. Kanada-En'yo, Physics Reports **432** (2006) 43

Core + valence neutron structures can be identified near the alpha-cluster decay threshold. Also, cluster states and structures can be seen in the collisions reactions near the Coulomb barrier, for example, in ^9Be , ^{12}C , $^{16,18}\text{O}$, ^{24}Mg nuclei.



Hyperspherical functions method for three body problem

Jacobi's vectors



$$\vec{R} = \vec{r}_3 - \vec{r}_1, \quad \vec{x} = \sqrt{\frac{M}{m_0 x_0^2}} \vec{R}, \\ \vec{r} = \vec{r}_2 - \frac{\vec{r}_1 + \vec{r}_3}{2}, \quad \vec{y} = \sqrt{\frac{\mu}{m_0 x_0^2}} \vec{r}. \quad (1)$$

$$M = \frac{m_1 m_2}{m_1 + m_2} \quad \mu = \frac{m_3 (m_1 + m_2)}{m_1 + m_2 + m_3} \quad (2)$$

$$x_0 = 1 \text{ fm}, \quad m_0 = 1 \text{ a.u.m.}$$

Hyperspherical coordinates
 $x = \rho \cos \alpha, \quad y = \rho \sin \alpha$

Replacing wave function for the ground state ψ_0 by a series of hyperspherical functions,

$$\psi_0(\alpha, \theta, \rho) = \sum \chi_K^{l_x}(\rho) \rho^{-5/2} \Phi_{K00}^{l_x l_x}(\alpha, \theta) \quad (3)$$

$$l_x = 0, 2, 4, \dots; \quad n = 0, 1, 2, \dots; \quad K = 2l_x + 2n;$$

Functions $\chi_K^{l_x}(\rho)$ are found from system of hyperradial equations $l_{max} = 12, n_{max} = 12$

$$\frac{d^2}{d\rho^2} \chi_K^{l_x}(\rho) + \left[2E b_0 - \frac{1}{\rho^2} (K+3/2)(K+5/2) \right] \chi_K^{l_x}(\rho) = \\ = 2b_0 \sum_{K' l_x'} \tilde{U}_{KK'}^{l_x l_x'}(\rho). \quad (4)$$

Coefficient m_i of the cubic spline equals to the second derivative of hyperradial wave functions

$$\frac{d^2}{d\rho^2} \chi_K^{l_x}(\rho_i) = m_i \quad (5)$$

$$F_i = \chi_K^{l_x}(\rho_i) \quad (6)$$

The system of equations for the cubic spline

$$\mathbf{A}\mathbf{m} = \mathbf{HF} \quad (7)$$

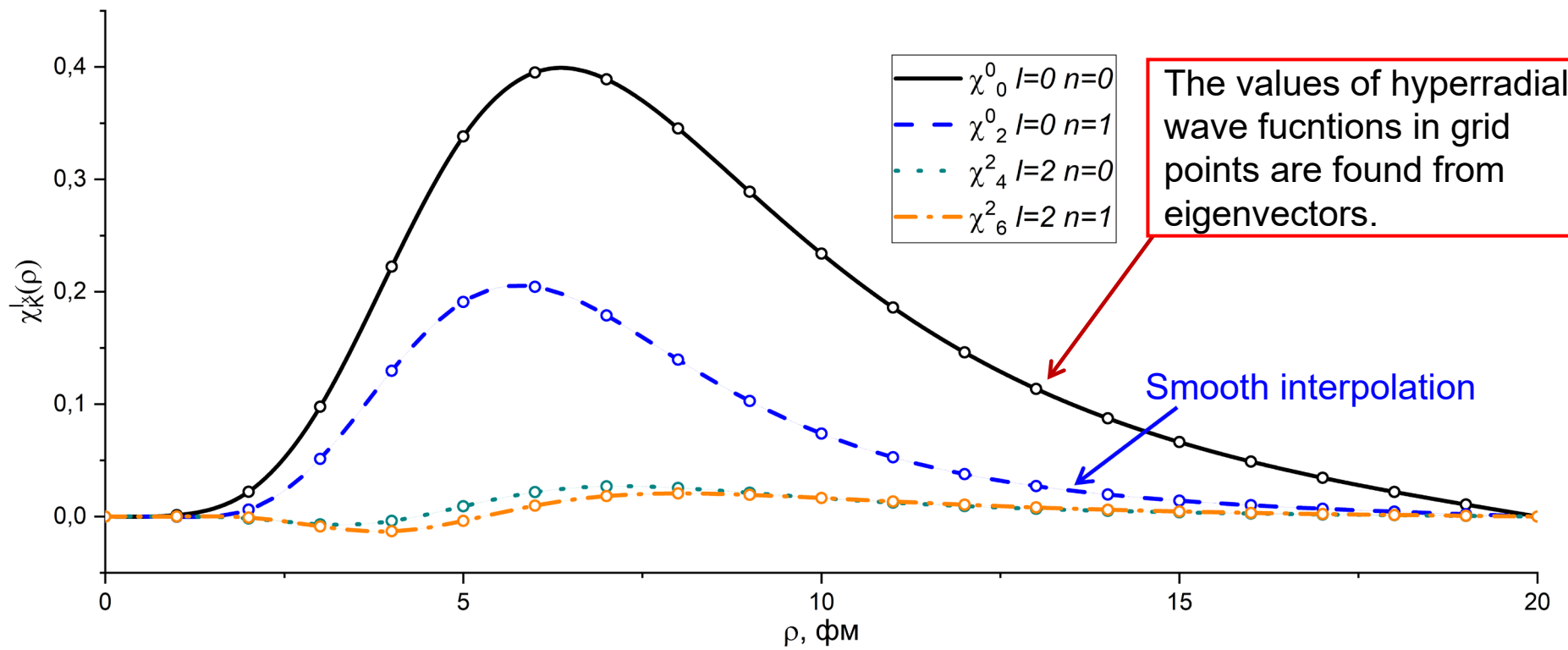
Matrices \mathbf{A} and \mathbf{H} can be found in
 [Marchuk G.I. Methods of Numerical Mathematics. -Springer NY, 1982]

$$\mathbf{BF} = \lambda \mathbf{F},$$

$$\mathbf{B} = -\mathbf{A}^{-1} \mathbf{HF} + \mathbf{WF}, \quad \lambda = \frac{2\mu}{\hbar^2} E. \quad (8)$$

The problem is reduced to the problem of eigenvalues and eigenvectors of matrix \mathbf{B}

Cubic spline interpolation allows to get smooth function between grid points



The example of spline interpolation of hyperradial wave functions $\chi_K^{l_x}$ ($n = 0, 1$; $l_x \equiv l = 0, 2$; $h = 1 \text{ fm}$, $\rho = [0, 20 \text{ fm}]$)

Interaction potential of alpha-particles

The potential of strong interaction $V_{\alpha-\alpha}$ is based on data of alpha-alpha scattering, known as Ali-Bodmer (AB) potential [1]

$$V_{\alpha-\alpha}^{(N)}(r) = v_1 \exp(-r^2/a_1^2) - v_2 \exp(-r^2/a_2^2) \quad (1)$$

Coulomb interaction $V_{\alpha-\alpha}^{(C)}(r)$ obtained from [1,2].

$$V_{\alpha-\alpha}^{(C)}(r, a_c, b_c) = a_c \cdot \operatorname{erf}(b_c r) / r \quad (2)$$

Potential with two Woods-Saxon's functions (2WS) has more parameters. It is important when describing experimental data [3]

$$V_{\alpha-\alpha}^{(N)}(r) = -U_{\alpha 1} f(r, B_{\alpha 1}, a_{\alpha 1}) + U_{\alpha 2} f(r, B_{\alpha 2}, a_{\alpha 2}) \quad (3)$$

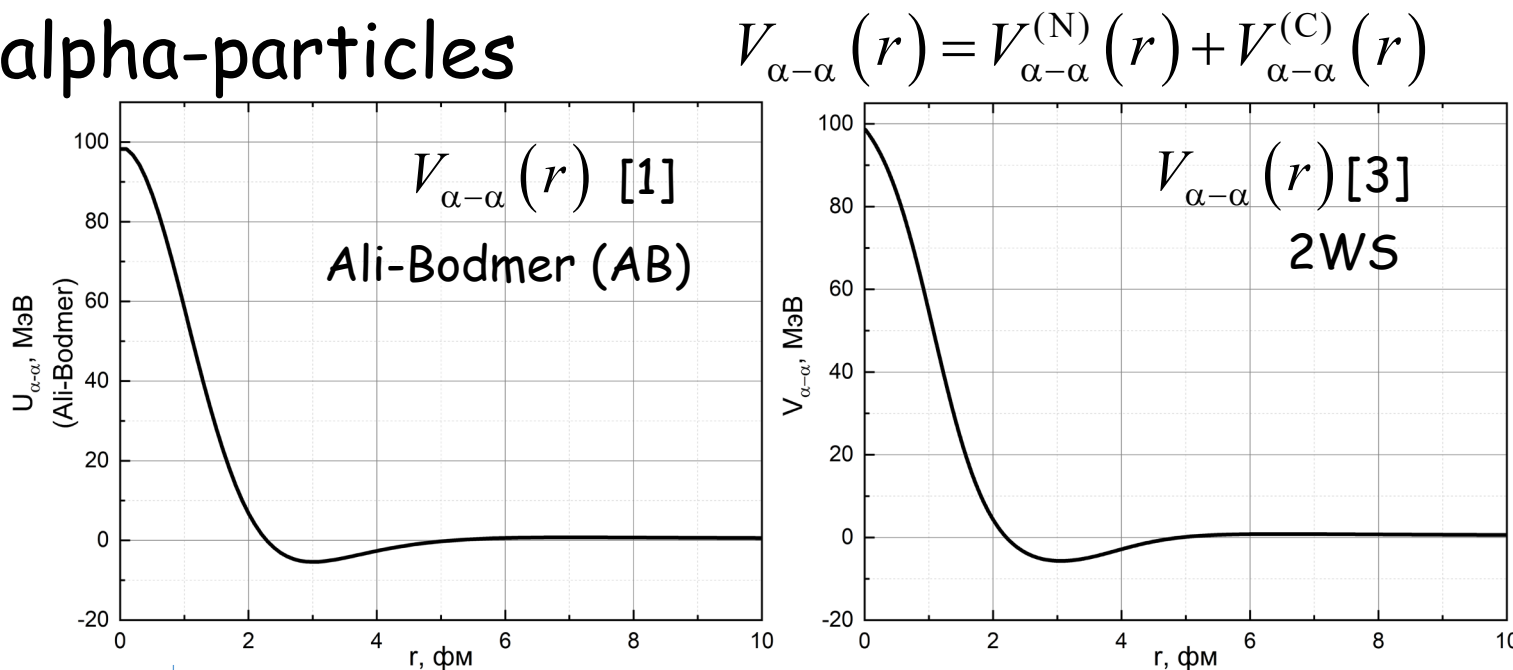
Wood-Saxon's type function $f(r, B, a)$

$$f(r, B, a) = \left[1 + \exp\left(\frac{r - B}{a}\right)^{-1} \right] \quad (4)$$

[1] S. Ali, A.R. Bodmer, Nucl. Phys. **80**, 99 (1966).

[2] H. Suno, Y. Suzuki, P. Descouvemont, Phys. Rev. C **91**, 014004 (2015).

[3] V.V. Samarin, Study of spatial structures in α -cluster nuclei, Eur. Phys. J. A, **58**, 117 (2022).



Alpha-alpha scattering potentials AB (left) and 2WS (right) are almost the same.

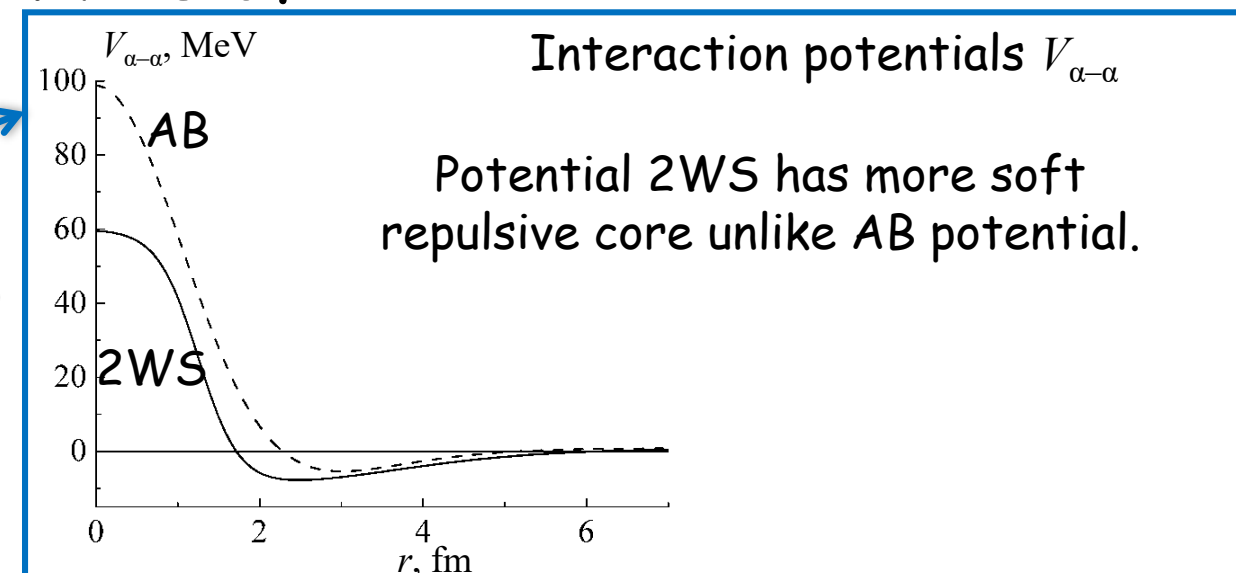
It is known that potential AB doesn't fit for describing bound energy of alpha-cluster nuclei, for example ^{12}C . Because of that, potential 2WS was used for describing interaction of alpha-clusters.

Selection of parameters of α - α interaction potential for making an agreement with experimental properties of alpha-cluster nucleus ^{12}C (3α)

1. To get an agreement with experimental data parameters of potential 2WS of ^{12}C **were modified**. Obtained **charge distribution** and separation energy into 3α -particles of ^{12}C are close to the experimental one.
2. After α -particle separation in ^{12}C , unbound nucleus ^{8}Be is formed. Because of that, the ground state energy was obtained $E_0 = -7.272$ MeV that is close to experimental value of α -particle separation of ^{12}C $E_s = 7.366$ MeV [1] ($E_0 \approx -E_s$).
3. Calculated root-mean-square (rms) charge radii is also close to the experimental one

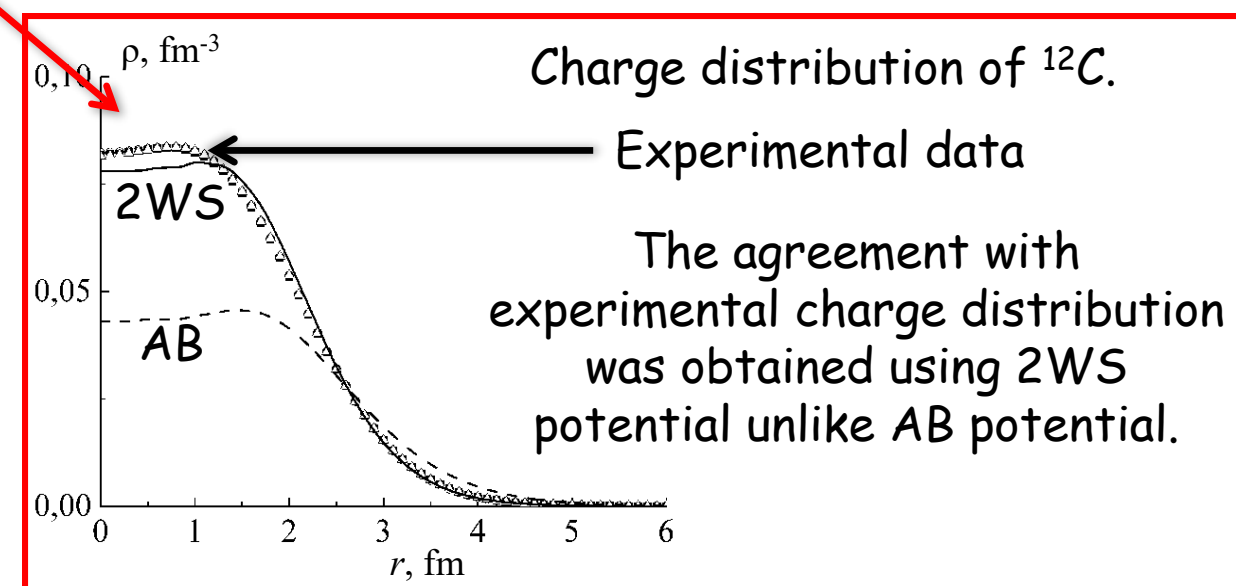
$$\langle r_C^2 \rangle_{\text{theor}}^{1/2} = 2.774 \text{ fm}, \quad \langle r_C^2 \rangle_{\text{exp}}^{1/2} = 2.47 \text{ fm}.$$

The difference occurs because of the errors in calculation the charge distribution at the region of large radii, where the charge density is low.



Interaction potentials $V_{\alpha-\alpha}$

Potential 2WS has more soft repulsive core unlike AB potential.



Charge distribution of ^{12}C .

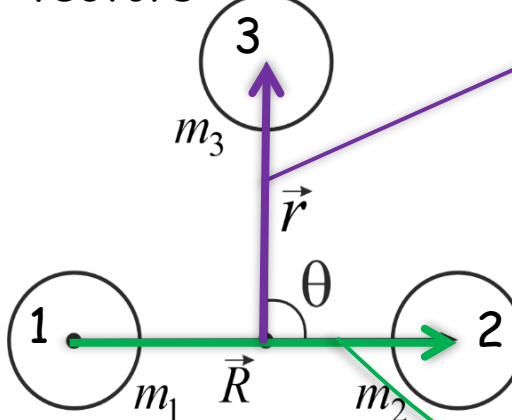
Experimental data

The agreement with experimental charge distribution was obtained using 2WS potential unlike AB potential.

The probability density for the ground state of alpha-cluster nucleues

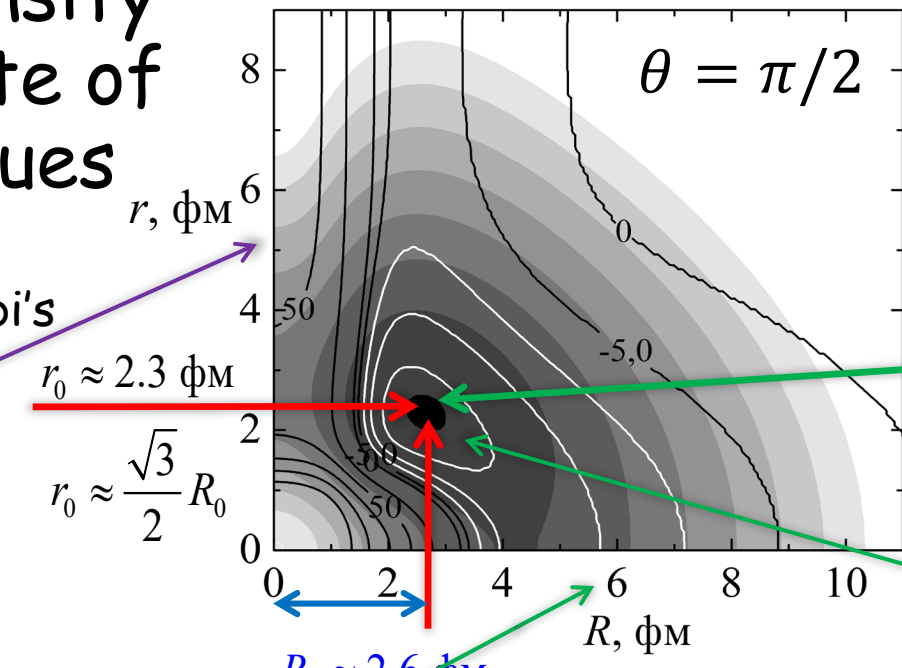
^{12}C (logarithmic scale)

In different positions of Jacobi's vectors

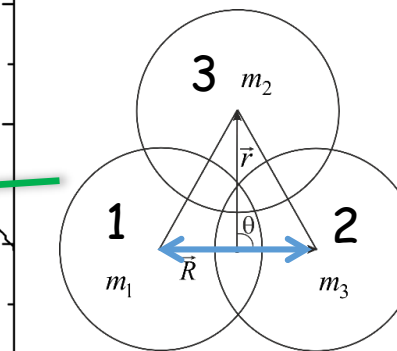


The softening of the repulsive core leads to overlapping of pure alpha-cluster structure.

Charge distribution and rms radii $\langle r_C^2 \rangle_{\text{theor}}^{1/2}$ calculated as average for all positions of vectors \vec{R} and \vec{r} .

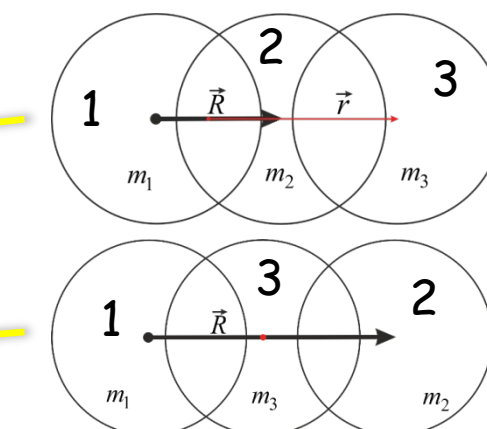
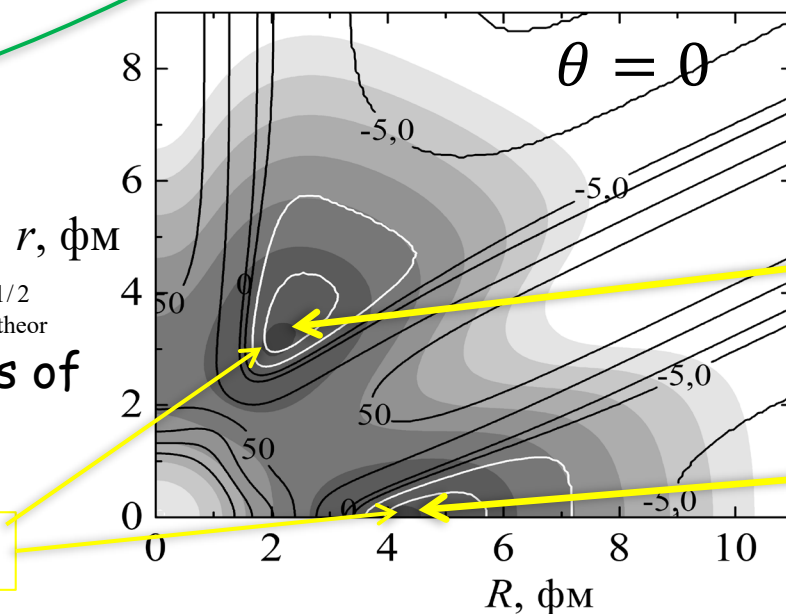


Positions of alpha-clusters, radii of alpha-clusters was chosen as rms radii of ^{4}He - 1.67 fm.



Triangular configuration

The most probable configuration is triangular, when alpha-clusters are located at the vertices of equilateral triangle with length of sides ~ 2.6 fm.



Linear configuration

Less probable configurations

Selection of parameters of α - α interaction potential for making an agreement with experimental properties of alpha-cluster nucleus ${}^6\text{Li}$ (α -n-p)

The nuclear part of the nucleon-nucleon interaction may be described by the effective pairwise central soft-core Afnan-Tang (A-T) potential [7] for a triplet state (t) and for a singlet (s) state

$$V_{t,s}(r) = \sum_{i=1}^3 v_i^{(t,s)} \exp(-\beta_i^{(t,s)} r^2)$$

We using effective nucleon-nucleon pseudopotentials $V_{\alpha\text{-n}}$ and $V_{\alpha\text{-p}}$ in calculations [1]. The pseudopotentials do not take into account the data on phase shifts, but their forms are similar to α - α and nucleon-nucleon potentials. The parameters of the pseudopotentials were determined from the condition of equality of the calculated and experimental values of the ground state energies for systems α -cluster + nucleons.

$$V_{\alpha-N}^{(N)}(r) = -u_1 f(r, B_1, a_1) + u_2 f(r, B_2, a_2) - u_3 f(r, B_3, a_3) f(r, B_4, a_4),$$

$$f(r, B, a) = \left[1 + \exp\left(\frac{r - B}{a}\right) \right]^{-1}, \quad V_{\alpha\text{-n}}(r) = V_{\alpha-N}^{(N)}(r), \quad V_{\alpha\text{-p}}(r) = V_{\alpha-N}^{(N)}(r) + V_{\alpha-p}^{(C)}(r)$$

The parameters of the SX variant [1] of the A-T-potential

	$v_1(\text{MeV})$	$v_2(\text{MeV})$	$v_3(\text{MeV})$	$\beta_1(\text{fm}^{-2})$	$\beta_2(\text{fm}^{-2})$	$\beta_3(\text{fm}^{-2})$
t	500	-102	-2	11.41	0.625	0.141
s	500	-102	-2	4.15	0.625	0.141

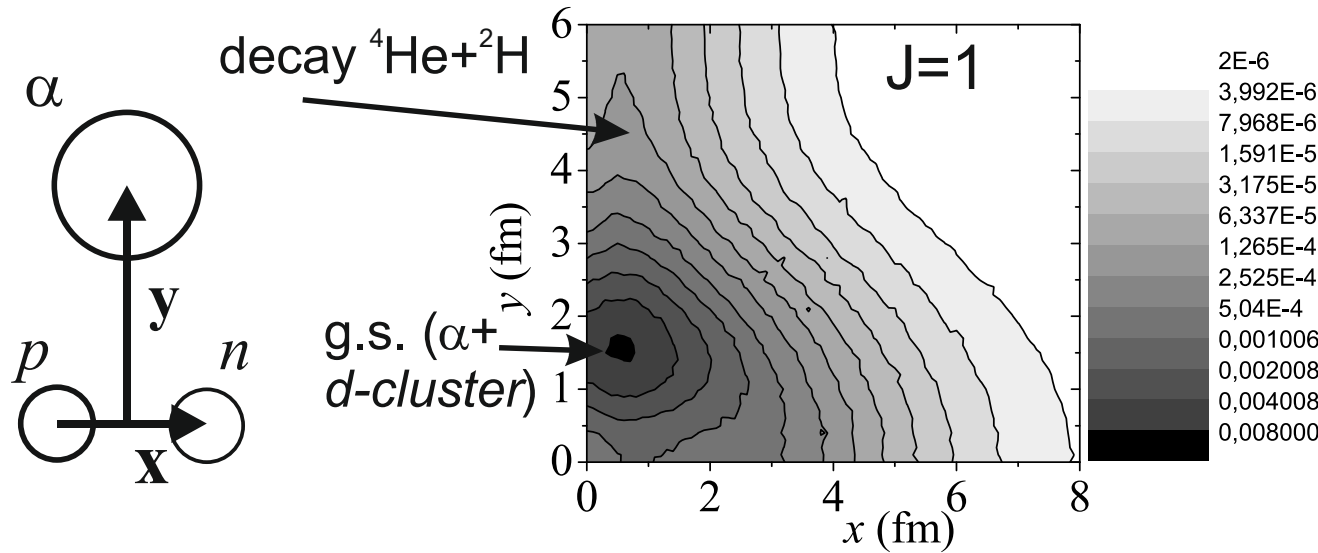
I	u_1 (MeV)	B (fm)	a (fm)
1	64.8	1.95	0.25
2	55.8	1.22	0.3
3	119	0.9	0.5
4	—	2.7	1

The probability density for the ground state of alpha-cluster nucleues ${}^6\text{Li}$

The ground state $J=1$:

$E_{\text{sep}} = 3.725 \text{ MeV}$ (to 3 particles α , p and n).

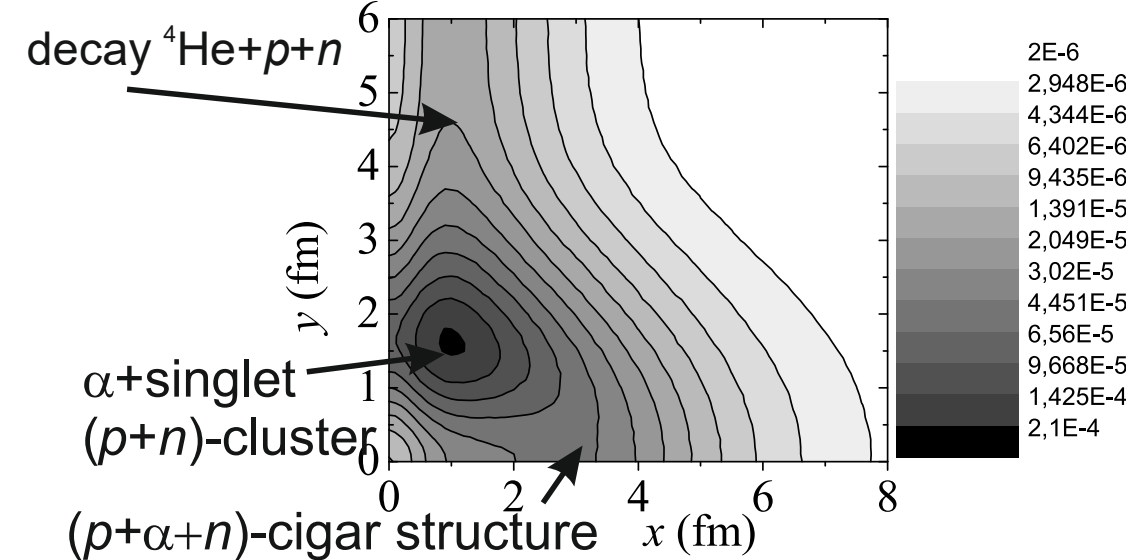
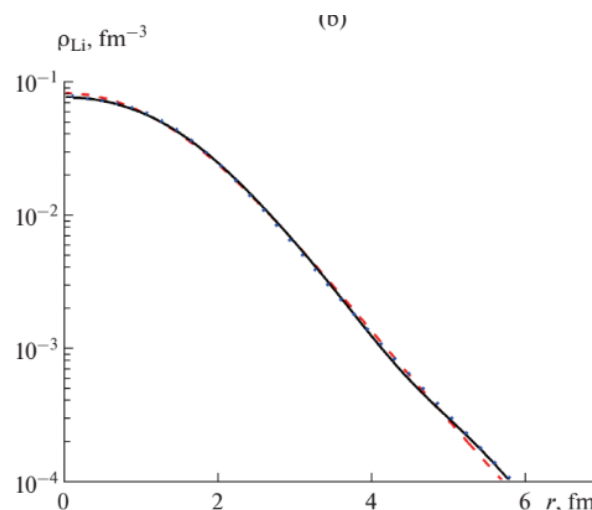
The calculated energy of the ground state with the triplet state of $(p+n)$ subsystem is -3.7 MeV .



The excited state $J=0$:

with $E_{\text{exc}} = 3.563 \text{ MeV}$, $E_{\text{sep}} = 0.162 \text{ MeV}$ (to 3 particles α , p and n) may be presented as the ground state with the singlet state of $(p+n)$ subsystem, calculated energy is -0.3 MeV .

Electric charge distribution density (in units of elementary charge) for the ground state of the ${}^6\text{Li}$ nucleus.



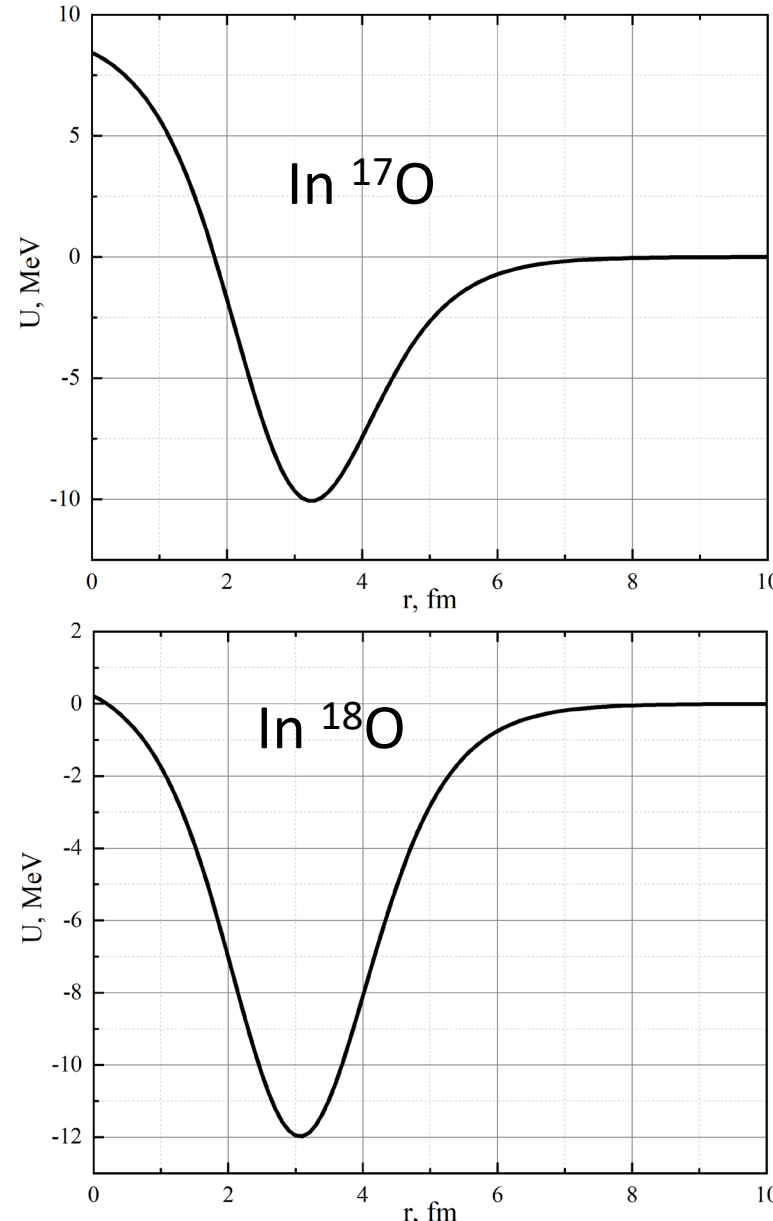
Core-nucleon potential in ^{17}O , ^{18}O

The two-body Schrodinger equation was also solved by spline-interpolation method. The calculated energy separation for ^{17}O is -4.01 MeV and the experimental value is 4.14 MeV. This potential gives the correct energy.



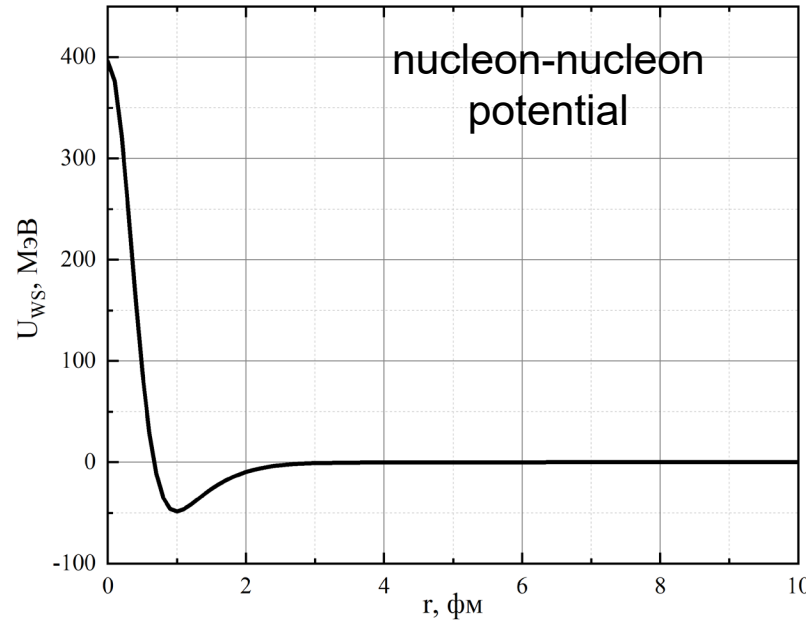
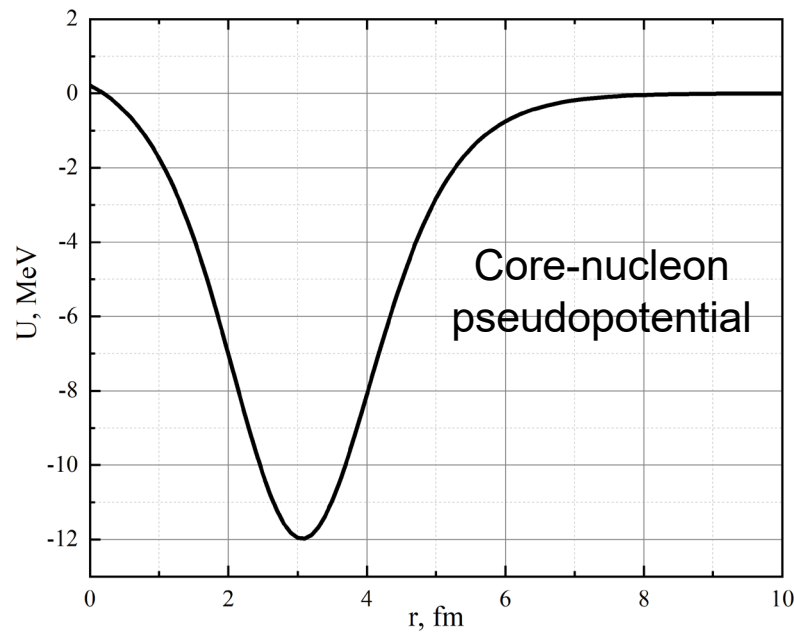
17	O
α - decay	-6358.67
β^- - decay	-2760.43
β^+ - decay	-9700.87
e-capture	-8678.87
1p - decay	-13781.67
2p - decay	-25259.91
1n - decay	-4143.06

The similar potential was used to calculate the separation energy of ^{18}O .

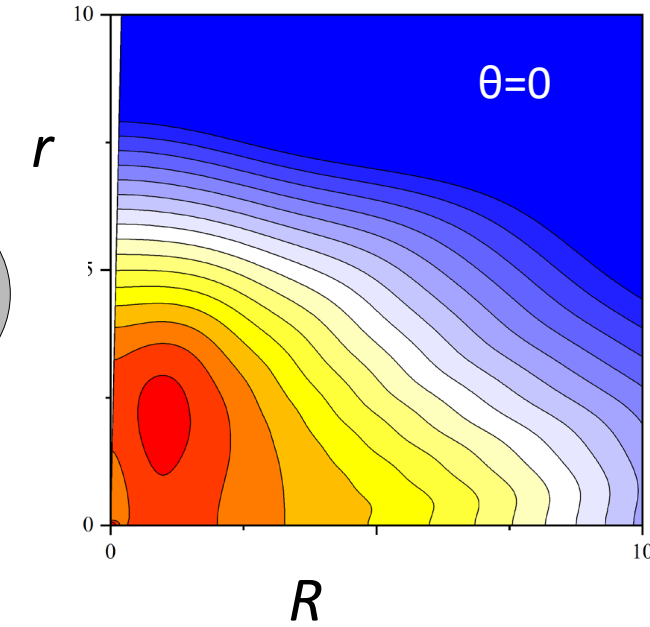
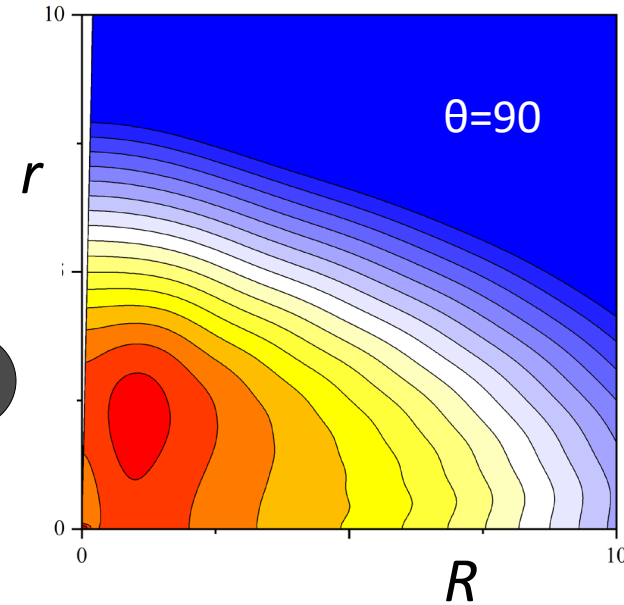
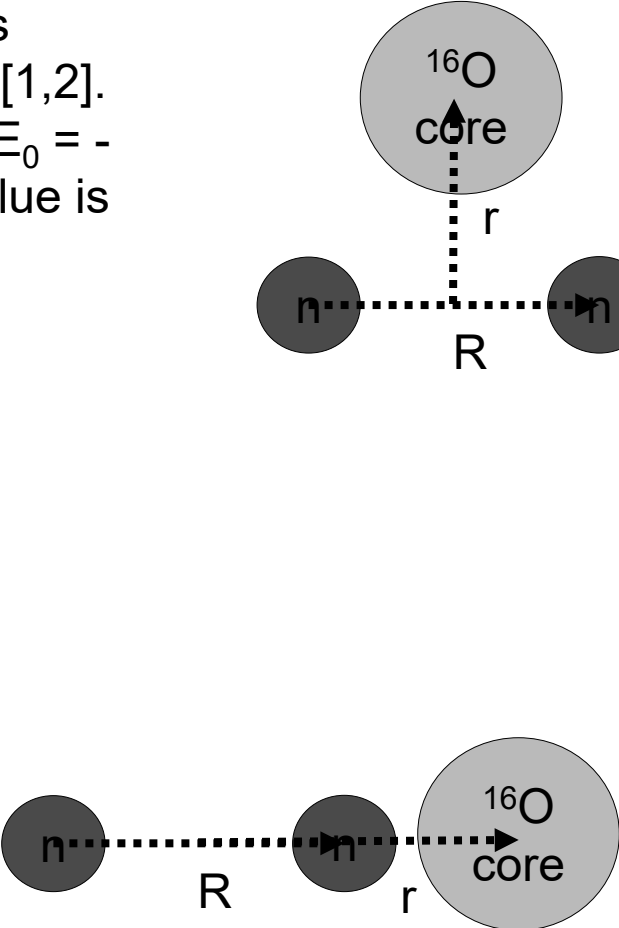
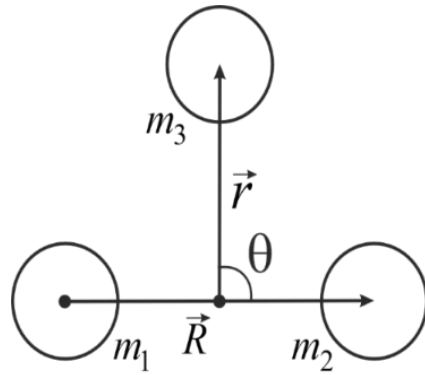


Nucleon–nucleon potentials for description of ^{18}O

Below we use the nucleon-nucleon potentials SX and α -nucleon pseudopotential to calculate of the ground state energies for system ^{18}O (core+ $n+n$).



Wave function of the ground state of the ^{18}O nuclei in the core+neutrons model is calculated hyperspherical functions [1,2]. For ^{18}O the energy of separation is $E_0 = -12.38$ MeV and the experimental value is 12.188 MeV.



1. V.V. Samarin, Eur. Phys. J. A, **58**, 117 (2022).

2. A.S. Bazhin, V.V. Samarin, Bull. Russ. Acad. Sci: Phys, **88**, 1177 (2024).

Feynman's path integrals (FPI) method

Feynman's approach [1] is not based on the Schrödinger equation, and the Lagrange method is used instead of Hamiltonian one [2]. The main object in the Feynman formulation is a propagator $K(q, t; q_0, t_0)$, which enables to express a wave function $\psi(q, t)$ in terms of its initial value $\psi(q_0; t_0)$ at the time $t = t_0$. Here q can stand for any dynamic variables describing our system at time t , and q_0 is the same variables at time t_0 .

$$\psi(q, t) = \int K(q, t; q_0, t_0) \psi(q_0, t_0) dq_0$$

The propagator $K(q, t; q_0, t_0)$ may be represented in the forms:

$$K(q, t; q_0, t_0) = \int K(q, t; q'', t'') K(q'', t''; q_0, t_0) dq''$$

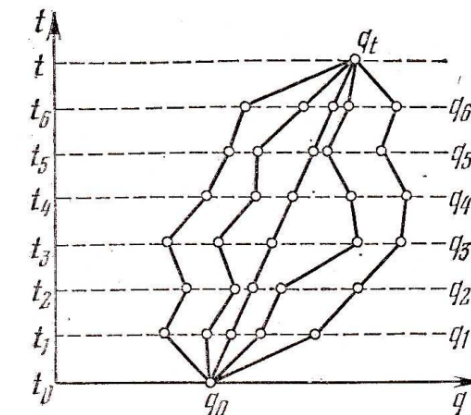
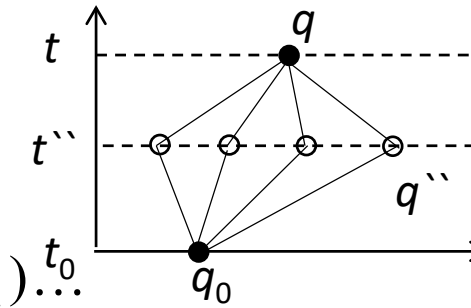
$$K(q, t; q_0, t_0) = \int \dots \int K(q, t; q_{N-1}, t_{N-1}) K(q_{N-1}, t_{N-1}; q_{N-2}, t_{N-2}) \dots$$

$$\dots K(q_2, t_2; q_1, t_1) K(q_1, t_1; q_0, t_0) dq_{N-1} dq_{N-2} \dots dq_1$$

1. R.P. Feynman, A.R.Hibbs, *Quantum Mechanics and Path Integrals* (McGraw-Hill, New York, 1965).

2. D. I. Blokhintsev, *Quantum Mechanics* (Springer, 1964);
QUANTUM MECHANICS (Chapter 25),
<https://vixra.org/pdf/2207.0018v1.pdf>

Д.И. Блохинцев, Основы квантовой механики. М.: Наука, 1983.



Particle trajectories which are subject for integration over in the Markov chain. The time interval $(t_0; t)$ is broken down into seven subintervals, q the particle coordinate.

The propagator in Feynman's path integrals method has properties:

The propagator K for an infinitesimal time interval $\Delta t = t_{k+1} - t_k$ is taken as

$$K(x_{k+1}, t_{k+1}; x_k, t_k) = C \exp \left\{ \frac{i}{\hbar} \left[\frac{m}{2} \left(\frac{x_{k+1} - x_k}{\Delta t} \right)^2 - V(x_k) \right] \Delta t \right\}, \quad C = \left(\frac{m}{2\pi i \hbar \Delta t} \right)^{1/2}; \quad K = \delta(x_{k+1} - x_k), \quad \Delta t \rightarrow 0.$$

The propagator K for the total time interval $(t_0; t)$ is:

$$K(x, t; x_0, t_0) = \lim_{N \rightarrow \infty} \int \dots \int \exp \left\{ \frac{i}{\hbar} \left[\frac{m}{2} \left(\frac{x_{k+1} - x_k}{\Delta t} \right)^2 - V(x_k) \right] \Delta t \right\} C^{N/2} dx_1 dx_2 \dots dx_{N-1},$$

The propagator $K(x, t; x_0, t_0)$ is a matrix element of the evolution operator

$$K(q, t; q_0, t_0) = \langle q | \hat{U}(t, t_0) | q_0 \rangle = \langle q | \exp \left[-\frac{i}{\hbar} \hat{H}(t - t_0) \right] | q_0 \rangle$$

$$K(q, t; q, 0) = \sum_n |\langle n | q \rangle|^2 \exp \left[-\frac{i}{\hbar} E_n t \right] = \sum_n |\psi_n(q)|^2 \exp \left[-\frac{i}{\hbar} E_n t \right]$$

$$\int_{-\infty}^{\infty} K(q, t; q, 0) dq = \sum_n \int_{-\infty}^{\infty} |\psi_n(q)|^2 dq \exp \left[-\frac{i}{\hbar} E_n t \right] = \sum_n \exp \left[-\frac{i}{\hbar} E_n t \right]$$

Feynman's path integrals method in imaginary time $t = -i\tau$ [1]

$$K(q, -i\tau; q, 0) \equiv K_E(q, \tau; q, 0) = \sum_n |\psi_n(q)|^2 \exp\left[-\frac{i}{\hbar} E_n(-i\tau)\right] = \sum_n |\psi_n(q)|^2 \exp\left[-\frac{1}{\hbar} E_n \tau\right] \approx |\psi_0(q)|^2 \exp\left[-\frac{1}{\hbar} E_0 \tau\right], \tau \rightarrow \infty$$

$$\int_{-\infty}^{\infty} K_E(q, \tau; q, 0) dq = \sum_n \int_{-\infty}^{\infty} |\psi_n(q)|^2 dq \exp\left[-\frac{1}{\hbar} E_n \tau\right] = \sum_n \exp\left[-\frac{1}{\hbar} E_n \tau\right] \approx \exp\left[-\frac{1}{\hbar} E_0 \tau\right], \tau \rightarrow \infty \quad (1)$$

The formula (1) is used to obtain the ground state energy E_0 as the slope of the linear part of the graph of $\ln K_E$ as a function of τ . The squared modulus of the ground state wave function $|\psi_0(q)|^2$ in the points q of the finite region corresponding to finite motion can be determined based on expression (1) at τ values in the linear part of the graph of dependence $\ln K_E(q, \tau; q, 0)$ on τ .

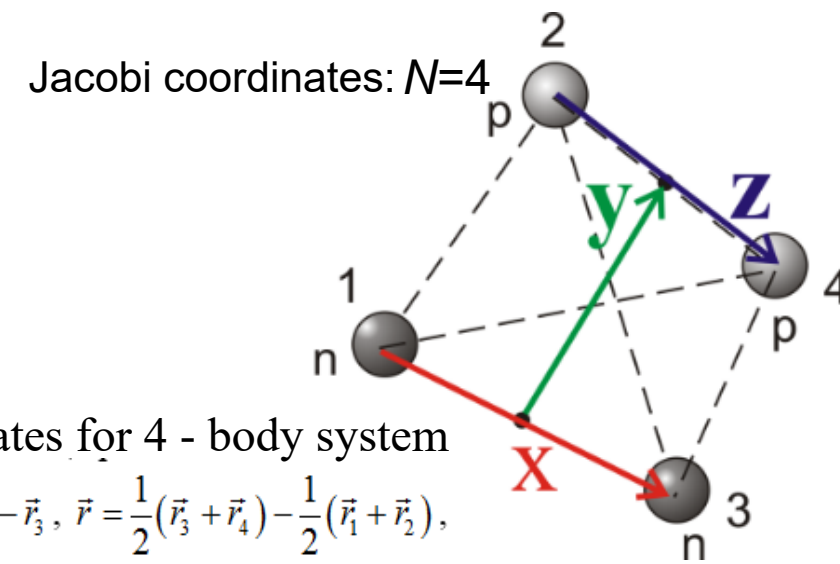
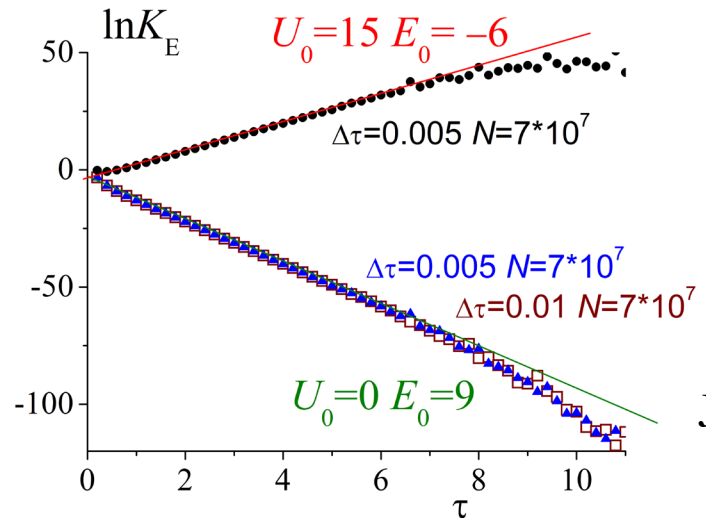
$$\ln K_E(q, \tau; q, 0) \approx \ln |\Psi_0(q)|^2 - E_0 \tau / \hbar, \tau \rightarrow \infty,$$

$$K_E(x, \tau; x, 0) = \lim_{N \rightarrow \infty} \int \dots \int \exp\left\{-\frac{1}{\hbar} \left[\frac{m}{2} \left(\frac{x_{k+1} - x_k}{\Delta \tau} \right)^2 + V(x_k) \right] \Delta \tau\right\} C^{N/2} dx_1 dx_2 \dots dx_{N-1}, \quad C = \left(\frac{m}{2\pi\hbar\Delta\tau} \right)^{1/2} \quad (2)$$

The values of the propagator (2) in Jacobi coordinates were calculated using algorithm proposed in [2, 3] based on the Monte–Carlo method and parallel calculations [4] using NVIDIA CUDA technology [5, 6] were performed mainly on the Heterogeneous Cluster of the Joint Institute for Nuclear Research [7]. Also, the calculations can be performed on CPU using parallel libraries (for example, OpenMP, IntelTBB).

1. E.V. Shuryak, O.V. Zhirov, Nucl. Phys. B 242, 393 (1984); Э. В. Шуряк, УФН 143, 309 (1984).
2. V.V. Samarin, M.A. Naumenko, Phys. Atom. Nucl. 80, 877 (2017).
3. V.V. Samarin, Study of spatial structures in α -cluster nuclei, Eur. Phys. J. A, 58, 117 (2022).
4. M.A. Naumenko, V.V. Samarin, Supercomp. Front. Innov. 3, 80 (2016)
5. NVIDIA CUDA, <http://developer.nvidia.com/cuda-zone/>
6. J. Sanders, E. Kandrot, *CUDA by Example: An Introduction to General-Purpose GPU Programming* (Addison-Wesley, New York, 2011)
7. Heterogeneous Cluster, Joint Institute for Nuclear Research, <http://hybrilit.jinr.ru/>

The capabilities of the FPI method is tested for exactly solvable oscillatory models with $N=4$



The slope of resulting straight lines equals
the energy of the ground state

$$\ln K_E(q, \tau; q, 0) \approx \ln |\Psi_0(q)|^2 - E_0 \tau, \quad \tau \rightarrow \infty, \quad (\hbar = 1)$$

FPI Monte-Carlo calculations
with statistics $n=10^7$.

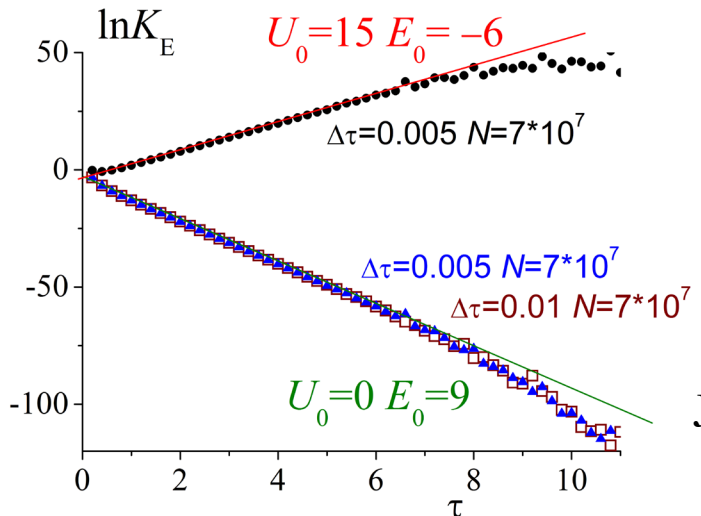
$$m_i = 1, \quad i = 1, \dots, N; \quad U = -U_0 + \sum_{i < j} \frac{\omega^2}{2} r_{ij}^2,$$

Exact E_0 value:

$$E_0 = -U_0 + \hbar \omega \frac{3}{2} (N-1) \sqrt{N}, \quad \omega = 1, \quad \hbar = 1.$$

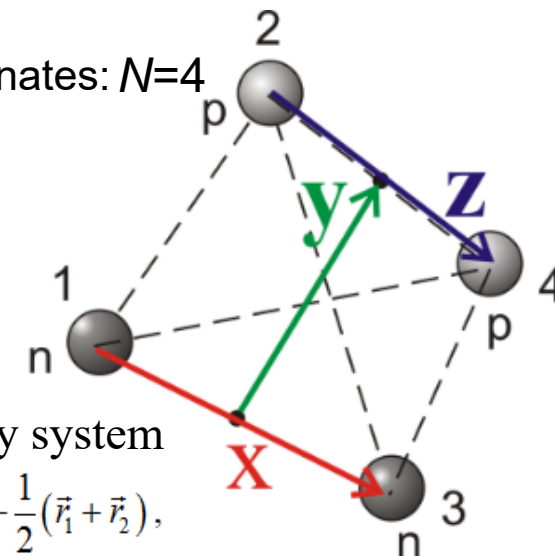
To demonstrate the capabilities of this
method, we use it for harmonic oscillatory
systems (exactly solvable) with exact
expressions for the ground state energy.

The capabilities of the FPI method is tested for exactly solvable oscillatory models with $N=4$



Jacobi coordinates for 4 - body system

$$\vec{R}_1 = \vec{r}_2 - \vec{r}_1, \vec{R}_2 = \vec{r}_4 - \vec{r}_3, \vec{r} = \frac{1}{2}(\vec{r}_3 + \vec{r}_4) - \frac{1}{2}(\vec{r}_1 + \vec{r}_2),$$



The slope of resulting straight lines equals
the energy of the ground state

$$\ln K_E(q, \tau; q, 0) \approx \ln |\Psi_0(q)|^2 - E_0 \tau, \quad \tau \rightarrow \infty, \quad (\hbar = 1)$$

One can see that the FPI method yields the exact values of the ground state energy with small uncertainties, which makes it possible to use this method in calculations of the ground state energies for nuclear N -body systems with $N > 3$.

$$m_i = 1, i = 1, \dots, N; \quad U = -U_0 + \sum_{i < j} \frac{\omega^2}{2} r_{ij}^2,$$

Exact E_0 value:

$$E_0 = -U_0 + \hbar \omega \frac{3}{2} (N-1) \sqrt{N}, \quad \omega = 1, \quad \hbar = 1.$$

N, U_0	Exact value E_0	Calculated value E_0
$N = 4, U_0 = 15$	-6	-5.98 ± 0.02
$N = 4, U_0 = 0$	9	8.98 ± 0.02

Calculation the energy of separation from ^{160}O to 4-alpha

Calculation of K_E was performed using CUDA (float) with in-build generator of random numbers, the number of simulations is 10^7 .

Potential alpha-alpha

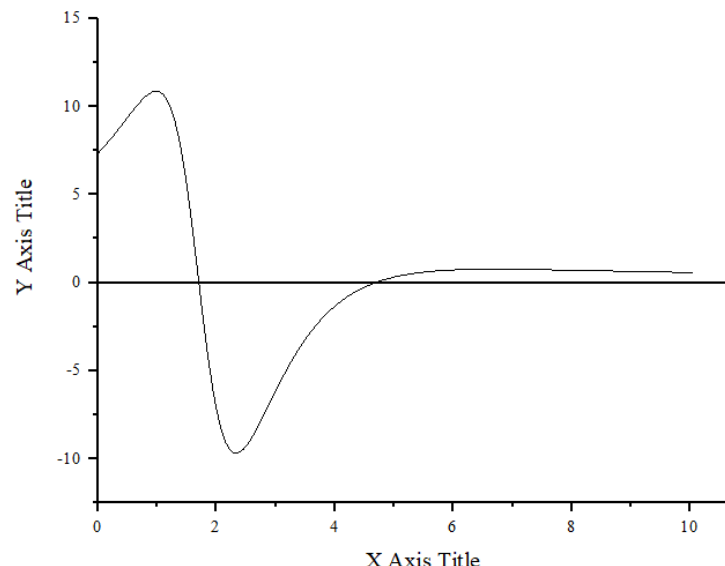
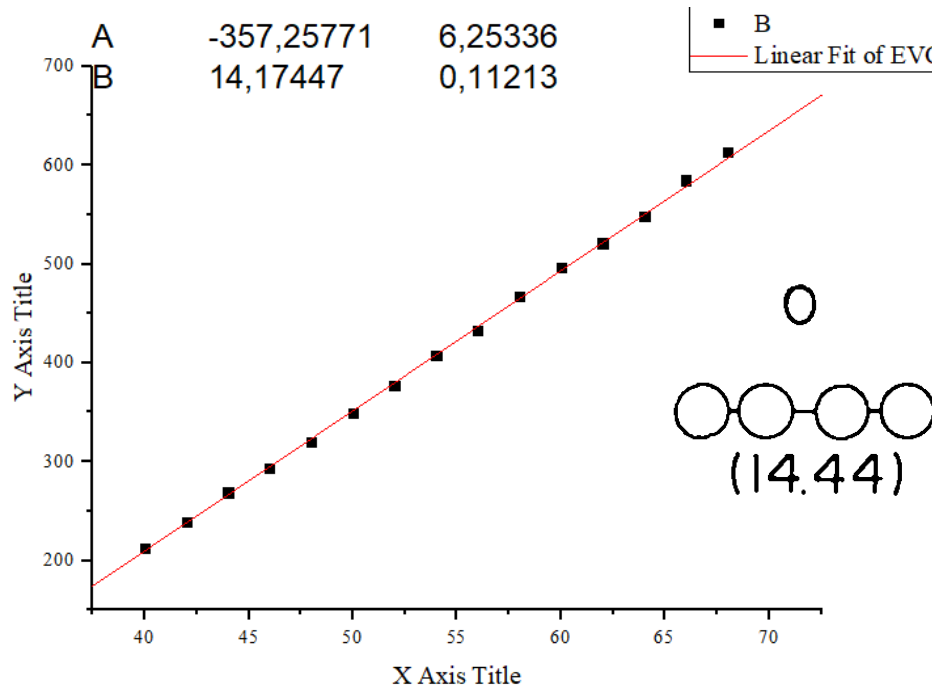
$$V_{\alpha-\alpha}^{(N)}(r) = -U_{\alpha 1} f(r; B_{\alpha 1}, a_{\alpha 1}) + U_{\alpha 2} f(r; B_{\alpha 2}, a_{\alpha 2})$$

$$f(r; B, a) = \frac{1}{1 + \exp\left(\frac{r - B}{a}\right)}$$

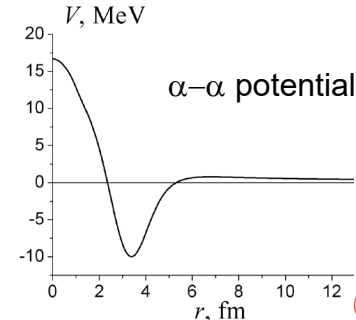
with parameters

$$U_{\alpha 1} = 39.8, B_{\alpha 1} = 1.93, a_{\alpha 1} = 0.8;$$

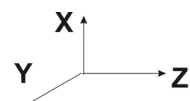
$$U_{\alpha 2} = 40.0, B_{\alpha 2} = 1.7, a_{\alpha 2} = 0.25;$$



Probability density for ground state of ^{16}O (4a) in α -cluster model using Feynman's path integrals



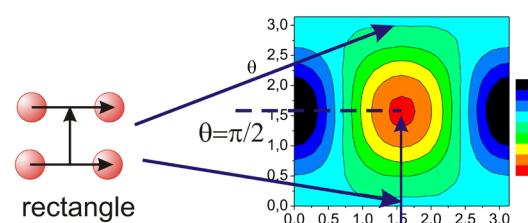
This region is important for the description of the one and two alpha-cluster transfer reactions and resonances.



X
 Y
 Z

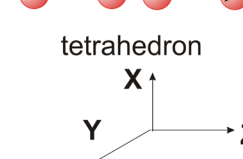
tetrahedron

square



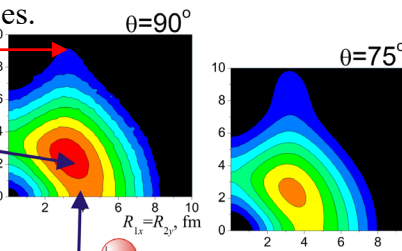
rectangle

rotation of R_2



Logarithmic scale

Calculation of charge density for ^{16}O is in process.



Jacobi coordinates
(R_1 , r , R_2)

parallel shift of R_2

$\alpha + ^{12}\text{C}$

α

R_1

r

θ

α

R_2

α

R_1

r

θ

<math

Метод функций Йоста

Метод функций Йоста основывается на переходе от дифференциального уравнения второго к двум дифференциальным уравнениям первого порядка, с помощью сферических функций

Бесселя/Неймана

$$\left[\frac{d^2}{dr^2} + k^2 - \frac{\ell(\ell+1)}{r^2} \right] \phi_\ell(E, r) = V(r) \phi_\ell(E, r),$$

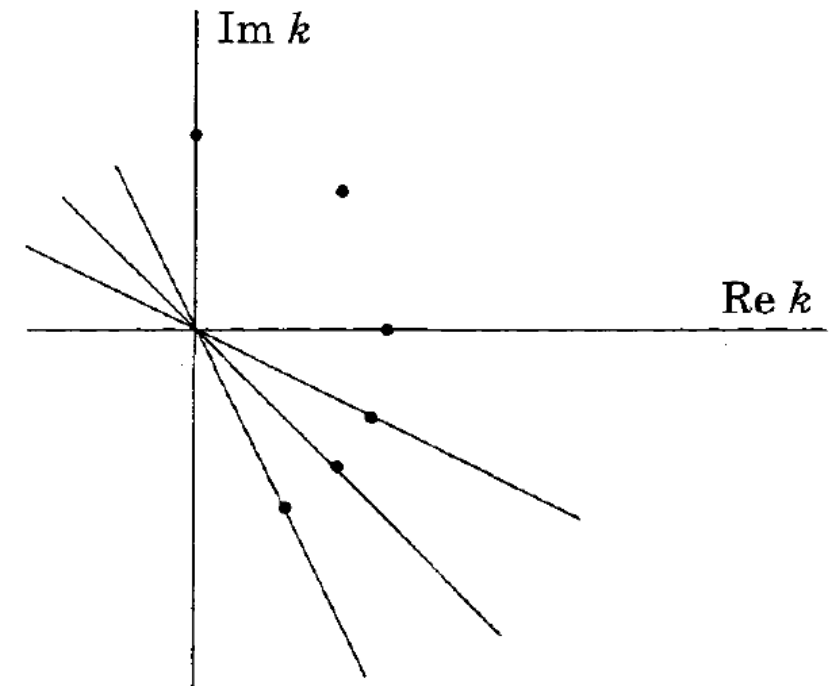


$$W_\ell^{(\text{in})}(E, r) = h_\ell^{(-)}(kr) |$$

$$W_\ell^{(\text{out})}(E, r) = h_\ell^{(+)}(kr)$$

$$\partial_r F_\ell^{(\text{in})} = -\frac{h_\ell^{(+)}(kr)}{2ik} V(r) \left[h_\ell^{(-)}(kr) F_\ell^{(\text{in})} + h_\ell^{(+)}(kr) F_\ell^{(\text{out})} \right]$$

$$\partial_r F_\ell^{(\text{out})} = -\frac{h_\ell^{(-)}(kr)}{2ik} V(r) \left[h_\ell^{(-)}(kr) F_\ell^{(\text{in})} + h_\ell^{(+)}(kr) F_\ell^{(\text{out})} \right]$$



Начальные условия, для решения системы дифференциальных уравнений

$$F_\ell^{(\text{in})}(E, 0) = F_\ell^{(\text{out})}(E, 0) = \frac{1}{2}$$

Участие в конференциях

1. 7th International Conference on Particle Physics and Astrophysics

Bazhin A.S. STUDY OF THE STRUCTURE OF ^{12}C AND ^6Li NUCLEI IN THE ALPHA-CLUSTER MODEL BY HYPERSPHERICAL FUNCTIONS, 2024.

Сайт конференции <https://indico.particle.mephi.ru/event/436/>

2. 28th International Scientific Conference of Young Scientists and Specialists (AYSS-2024)

Bazhin A.S. Study of nuclei structure in alpha-cluster model by hyperspherical functions using cubic spline interpolation, 2024.

Сайт конференции <https://indico.jinr.ru/event/4343/overview>

3. South Africa - JINR Workshop on Theoretical and Computational Physics

Bazhin A.S. Study of the structure of nuclei in the alpha-cluster model by hyperspherical functions method, 2025.

Сайт конференции <https://indico.jinr.ru/event/5349/overview>

4. LXXV International Conference «NUCLEUS – 2025. Nuclear physics, elementary particle physics and nuclear technologies»

Bazhin A.S. Study of the structure of $^{16,18}\text{O}$ nuclei in the alpha-cluster model by hyperspherical functions and Feynman's path integrals, 2025.

Сайт конференции <https://indico.jinr.ru/event/4343/overview>

Статьи

1. *Известия РАН Серия физическая том 88, номер 8, 2024.*

A.S. Bazhin and V.V. Samarin Study of the Structure of the ${}^9\text{Be}$ Nucleus in the Alpha-Cluster Model by the Method of Hyperspherical Functions. Bulletin of the Russian Academy of Sciences: Physics, 2024, Vol. 88, No. 8, pp. 1177–1184. **DOI:** [10.1134/S1062873824707281](https://doi.org/10.1134/S1062873824707281)

2. (Принято к опубликованию) *Известия РАН Серия физическая том 89, номер 8, 2025.*

A.S. Bazhin and V.V. Samarin "Study of the Structure of ${}^{12}\text{C}$ and ${}^6\text{Li}$ Nuclei in the Alpha-Cluster and Shell Models". Bulletin of the Russian Academy of Sciences: Physics, 2025, Vol. 89, No. 8, pp. 1273–1283. **DOI:** [10.1134/S1062873825712048](https://doi.org/10.1134/S1062873825712048)

3. (В планах) *Известия РАН Серия физическая*

A.S. Bazhin and V.V. Samarin "Исследование структуры ядер ${}^{18}\text{O}$ И ${}^{16}\text{O}$ в альфа-кластерной модели с использованием метода гипесферических функций и метода Фейнмана по траекториям"

Заключение

Проведены расчёты структуры ядер ^{12}C , ^6Li , ^{18}O и ^{16}O . Полученные расчёты согласуются с экспериментальными значениями (энергия основного состояния, зарядовый радиус, зарядовое распределение)

Разработаны программы на C++ для методов: функций Йоста и Фейнмана по траекториям. Данные методы будут использоваться в дальнейшем изучении структуры ядер, как связанных состояний, так и возбужденных состояний.

Спасибо за внимание!